Time-dependent density functional theory study of absorption spectra of metallocenes

Yong L. Li [a], Lei Han [b], Ye Mei [c], John Z.H. Zhang [c,d,*]

[a] School of Chemistry and Chemical Engineering, Nanjing University, 22 Hankou Road, Nanjing 210093, China
[b] Shanghai Institute of Organic Chemistry, Chinese Academy of Sciences, 345 Lingling Road, Shanghai 200032, China
[c] State Key Laboratory of Precision Spectroscopy, Department of Physics, East China Normal University, Shanghai 200062, China
[d] Department of Chemistry, New York University, New York, NY 10003, United States

ARTICLE INFO

ABSTRACT

Extensive TDDFT calculations with various combinations of functionals are carried out to compute low-lying excited states of ferrocene. The combined functional and basis set approach TD-PBE0/6-311++G(d,p) is found to be well-behaved in the calculation of excited states. This choice of functional/basis set can give correct ground-state geometries, excitation energies, absorption spectra, and correct symmetry sequence of low level unoccupied molecular orbitals. This method is applied to the calculation of excitation energies of bis(benzene)chromium and four derivatives of ferrocene and the results are accurate within 0.3 eV. The current study implies that the combination TD-PBE0/6-311++G(d,p) can be used to compute excited state properties of other transition metal complexes.

© 2009 Elsevier B.V. All rights reserved.

1. Introduction

Time-dependent density functional theory (TDDFT) provides an efficient means for computing excited states of chemicals, such as dye molecules and metallorganic compounds [1–7]. Metallocenes, especially ferrocene, are the most interesting prototypes of this type of compounds and have attracted significant interest [8]. TDDFT method is considered to be reliably accurate for calculating transition metal complex [9–12]. Although configuration methods such as CASSCF [13], CASPT2 [14], etc. could provide more accurate results, but their applications are limited because they either require much experience to deal with pitfalls such as the notorious intruder states [15] or need much more computer times. It is thus desirable to study excited state properties of metallocenes based on TDDFT approach. Of particular interest for us is to investigate the dependence of the computed molecular properties on specific functionals and basis sizes. It is known that the TDDFT may give relatively larger errors in predicting the d–d transition. In such cases, the method ΔSCF performs better [10]. But we will see that results from TDDFT are also acceptable. For all major transition types of metal centered (MC) metallorganic compounds, metal to ligand charge transfer (MLCT) and ligand to metal charge transfer (LMCT) are of valence type [10]. They can be reliably predicted by TDDFT than the Rydberg type transitions which are hard to be dealt with using TDDFT.

The first attempt to predict absorption spectrum of ferrocene is by Boulet et al. [5]. In that work, they used several functionals including B3LYP and calculated the first four excitations of D_{5d} ferrocene. Although the hybrid B3LYP functional is most popular to calculate diverse properties of various molecules, it has been noted that B3LYP is not ideal in calculating excited state properties of molecules [7,16] despite continued use of it [2,4,6]. We think it is important to perform a comparison study of existing functionals in their prediction of excited state properties molecules. It is also known that larger basis set does not necessarily result in more accurate results in DFT calculation [17]. It is thus possible to employ just moderate basis size to obtain results as accurate as that obtained from other post-Hartree–Fock methods such as CI, many-body perturbation etc. In those methods, large orbitals are needed. In our study we found that triple-ζ diffuse 6-311++G(d,p) [18] is sufficient to balance the accuracy and efficiency.

Another issue concerned is the symmetry sequence of virtual orbitals that are sensitive to functionals used, although they all give the same energy sequence for occupied orbitals. Even in two previous works, the reported symmetries of virtual orbitals are different [19,20]. As we will see below, different functionals and combined with pseudopotential would give different symmetry sequences of virtual orbitals. This difference of symmetry of virtual orbitals could confuse the specification of the transition type, and may be one of the resources of deviations of calculated excitation energies from experimental values.

---

* Corresponding author. Address: Department of Chemistry, New York University, New York, NY 10003, United States.
E-mail address: john.zhang@nyu.edu (J.Z.H. Zhang).

In this Letter, we first use ferrocene as the test system to study various molecular properties such as sensitivity of functional/basis combinations, ground state geometries, the first four lowest excitation energies, and the configuration of several low unoccupied orbitals. Based on the comparison study, we then apply the best functional/basis combination to calculate excitation energies of another metallocene, bis-(benzene) chromium. Further, we apply the desired combination to some derivatives of ferrocene, acetylferrocene (AcFc), hydroxyethylferrocene (HyFc), vinylferrocene (ViFc), and ethynylferrocene (EtFc).

2. Methods

All *ab initio* calculations are performed using GAUSSIAN 03 [21]. The initial structures ferrocene and other complexes are minimized. The excited states are computed with TDDFT. The functionals used in TDDFT calculations are B3LYP [22], PBE [23], BPW91 [24], and PBE0 [25]. The basis size used are TZVP [26], DZVP [27], 6-311G(d,p) [18], 6-311++G(d,p) [18,28], Ahlrichs-pVDZ [29] and aug-cc-pVTZ [30], respectively. We also employed pseudopotential Lanl2dz [31] in our calculation for purpose of comparison.

The theoretical excitation energies are calculated both *in vacuo* and in solution. To simulate the solvent environment, we used polarizable continuum model [32] with radii from United Atom Kohn–Sham topological model (UAKS). In calculations of four derivatives of ferrocene, the four degenerate excited states split to eight states. But only four or less absorption peaks are observed in experiment. So we simulated absorption profile using the SWIZARD program [33]. Gaussian functions with half-widths of 3000 cm^{-1} (a typical half-bandwidth for the complexes under consideration) is used in spectra simulation.

The four derivatives of ferrocene are prepared using methods in Refs. [34,35]. The excitation energies are measured by a UV–vis absorption spectra in dichloromethane solution on a UV-240 spectrometer from Shimadzu.

3. Results and discussion

3.1. Influence of functionals on structure of ferrocene

To calculate the absorption feature of ferrocene, we first need to obtain the minimum structure. The optimized structure of ferrocene is shown in Fig. 1 and selected geometric parameters are given in Table 1. The minimized structure is of D_{5h} symmetry which is a global minimum [36], in agreement with the prediction
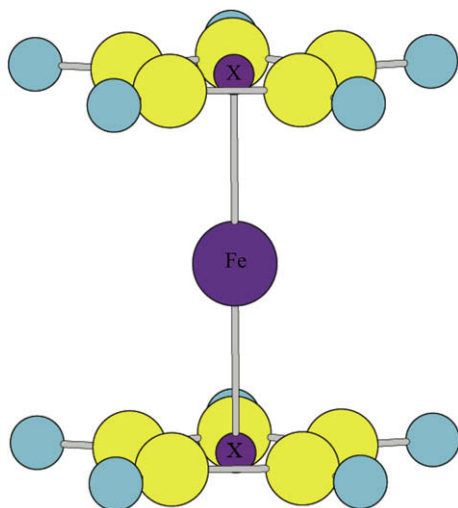
of Ref. [19]. The calculated structural properties of ferrocene are in good agreement with the available experimental data [37].

It is interesting to observe in our study that PBE0 and PBE calculations always underestimate the distance from Fe to the cyclopentadienyl ring (Cp) while B3LYP overestimates it. In contrast, BPW91 gives very accurate structural data. Overall, however, the deviations of structural parameters among these calculations are relatively small. This indicates that these functionals are reliable in predicting the structure of ferrocene.

3.2. Influence of functionals on electronic properties

Although Petit et al. claimed that pseudopotentials are suitable with TDDFT method, the order of MO (molecular orbital) energy levels derived from TDDFT + pseudopotential methods are different from those in Refs. [19,20], in which the sequence of orbitals of ferrocene was determined by DFT with diverse set of functionals and full electron basis. For example, if we use Lanl2dz pseudopotential, the MO energy level sequence from the lowest unoccupied MO (LUMO) to LUMO+3 is $(E1'')$ $(E1')$ $(A2'')$ $(A1')$ rather than the correct configuration $(E1'')$ $(A1')$ $(E2')$ $(E2'')$. In Fig. 2, we can see that the energy sequence of orbitals from PBE0 + pseudopotential calculation is quite different from PBE0 calculation with full electron basis. In Fig. 2, we can see that energy sequence of virtual orbitals from PBE0 + full electron basis calculation is very close to that of Refs. [20,19]. Although there is slight difference at two near-degenerate levels, $3E2''$ and $4E2'$, but it does not affect the excitation energy and the specification of the transition type.

Table 2 shows that the symmetry of virtual orbitals from B3LYP and BPW91 are different from Ref. [20] and the group theory calculations below. In the next section, one can see the absorption energies are quite similar as that from PBE0 calculation, this because in TDDFT, the energy gap between two orbitals is only the zeroth perturbation term, and the gap is different to the calculated excitation energy when the higher order corrections are added [10]. But the wrong symmetry sequence would make the specification of the absorption type difficult. And Head-Gordon [38] also pointed out that virtual orbitals of ground state are important in TDDFT calculations.

The absorption band could be assigned to two one-electron transitions:

$$(A1')^2(E2')^4 \rightarrow (A1')^2(E2')^3(E1''),$$
$$(A1')^2(E2')^4 \rightarrow (A1')^1(E2')^4(E1'').$$
(1)

The two representations of electronic dipole of D_{5h} group are $E1'$ and $A2''$ and the symmetries of transition moments are:

$$\langle \Psi_f|\mu|\Psi_i \rangle = \begin{Bmatrix} A1' \\ E2' \end{Bmatrix} \otimes \begin{Bmatrix} E1' \\ A2'' \end{Bmatrix} \otimes E1''$$

$$= \begin{Bmatrix} \begin{Bmatrix} A1'' + A2'' + E2'' \\ E1'' \end{Bmatrix} \\ \begin{Bmatrix} A1'' + A2'' + E1'' + E2'' \\ E1' + E2' \end{Bmatrix} \end{Bmatrix}.$$
(2)

Since there is no full-symmetric representation $(A1')$, transitions are dipole forbidden. But there are quadrupole transitions.

$$\langle \Psi_f|\mu|\Psi_i \rangle = \begin{Bmatrix} A1' \\ E2' \end{Bmatrix} \otimes \begin{Bmatrix} E1'' \\ A2' \end{Bmatrix} \otimes E1''$$

$$= \begin{Bmatrix} \begin{Bmatrix} A1' + A2' + E2' \\ E1' \end{Bmatrix} \\ \begin{Bmatrix} A1' + A2' + E1' + E2' \\ E1'' + E2'' \end{Bmatrix} \end{Bmatrix}.$$
(3)

Fig. 1. Representative 3D structures for ferrocene.

Table 1
Selected structural information of ferrocene.

Method	Basis	Pseudo[a]	Fe–X[b]	M–C	C–C	C–H	∠C–C–C	∠C–C–C–H
Experiment			1.658	2.056	1.429	1.08	108.00	–
PW91[c]	TZ2P(STO)	Frozen-core	1.647	2.048	1.432	1.09	108.00	0.840
B3LYP	6-311G(d,p)/Lanl2dz[d]	Lanl2dz	1.685	2.076	1.426	1.08	108.00	1.394
B3LYP	6-311G(d,p)/Lanl2dz[d]	Lanl2dz	1.685	2.076	1.426	1.08	108.00	1.414
B3LYP	6-311G(d,p)/Lanl2dz[d]	Lanl2dz	1.685	2.076	1.426	1.08	108.00	1.414
B3LYP	6-311G+(d,p)		1.685	2.076	1.426	1.08	108.00	1.133
B3LYP	6-311+G(d,p)		1.685	2.076	1.426	1.08	108.00	1.133
B3LYP	TZVP/DGDZVP2		1.655	2.050	1.422	1.08	108.00	1.657
B3LYP	6-311G(d,p)		1.675	2.068	1.426	1.08	108.00	1.138
PBE0	6-311G(d,p)/Lanl2dz[d]	Lanl2dz	1.643	2.040	1.422	1.08	108.00	1.806
PBE0	TZVP		1.655	2.050	1.422	1.08	108.00	1.657
PBE0	6-311G(d,p)		1.639	2.037	1.422	1.08	108.00	1.444
PBE0	6-311++G(d,p)		1.646	2.043	1.423	1.08	108.00	1.707
PBE0	TZVP/DGDZVP2		1.645	2.042	1.422	1.08	108.00	1.556
PBE0	Aug-cc-pVTZ/DGDZVP2[d]		1.640	2.037	1.420	1.08	108.00	1.654
PBE0	Aug-cc-pVTZ		1.650	2.045	1.420	1.08	108.00	1.547
PBE0 (PCM)	TZVP		1.655	2.050	1.422	1.08	108.00	1.881
PBE0 (PCM)	DGDZVP2		2.035	2.350	1.429	1.08	108.00	1.632
PBE	TZVP		1.647	2.050	1.435	1.09	108.00	1.230
PBE	TZVP/DGDZVP2[d]		1.637	2.042	1.435	1.09	108.00	1.250
bpw91	6-311G(d,p)/Lanl2dz[d]	Lanl2dz	1.644	2.048	1.436	1.09	108.00	1.146
bpw91	TZVP		1.654	2.056	1.435	1.09	108.00	0.912

[a] Blank denotes full electron basis is used.
[b] Å for distances and degree for angles.
[c] Data from Ref. [37].
[d] The basis of Fe atom is different from that of other atoms.
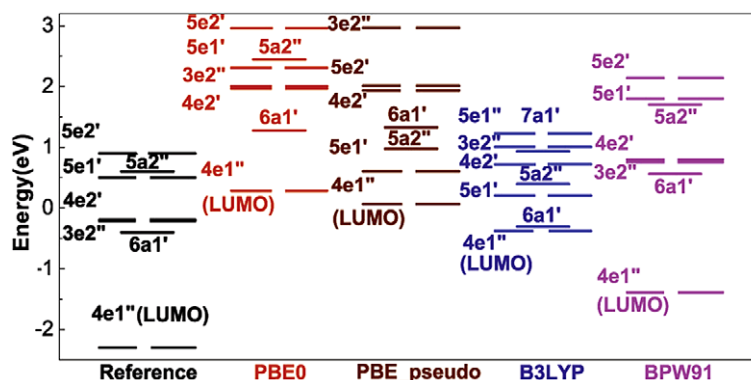
Fig. 2. Orbital energy levels from DFT calculations with four different functionals and from reference values given in Ref. [20].

Since both transitions are allowed, we can conclude that all the first four excitations of ferrocene are forbidden. However, there can be weak transition due to nonzero quadruples. The experiments both *in vacuo* and in solutions confirmed this [39].

3.3. Excited states of ferrocene

Although all the functionals used in our study could give decent geometry of ferrocene, results from Refs. [40,12,9,16] show that PBE0 generally gives more accurate excitation spectra. And the data in Table 2 which lists four calculated low-level excitation energies of ferrocene also convince this.

We also see that the energy of the first excited state is more sensitive to the basis size used. The four absorptions are mainly d–d transition. The first is a pure d–d transition ($3E2' \rightarrow 4E1''$) and is more sensitive to different orbitals used. The second and third transitions are two with MC transitions ($5A1' \rightarrow 4E1''$, $3E2' \rightarrow 4E1''$). In $5A1' \rightarrow 4E1''$, MC transition is dominant so they are less sensitive to different functionals and basis sets. It was suggested that ΔSCF method would be more accurate when dealing with d–d transition [10].

The absorption experiments on ferrocene are carried out either at solid state, in which the D_{5d} conformer is dominant, or in solution at room temperature, in which the D_{5h} conformer is prevalent. The extensive theoretical and experimental results on D_{5d} conformer of ferrocene can be found in Refs. [5,36,39,41–43], and experimental data in solution used in current study are from Ref. [39]. It is interesting to observe that the fourth excitation of D_{5d} ferrocene is similar as the third excitation of D_{5h}'s.

The most intensive absorption from our calculation is the second absorption, which is within the range of 450–460 nm, in excellent agreement with experimental value of 459 nm [39]. For taking account of the solvatochromism, we also calculated excitations of ferrocene in solution using PCM, obtaining the second absorption at 460 nm which is very close to the experimental value of 438 nm measured by one of the authors. Recent studies showed that absorption spectra from TDDFT calculations are generally within *Ca.* 0.3 eV [12,2,38]. Our results are similar or more accurate than this error estimated.

Table 2 also gives calculated absorption bands from B3LYP, BPW91, and PBE functionals. All of them have relatively large

Table 2
The four low-level excited states of D_{5h} ferrocene (unit: nm).

Method and basis Transition type	Pseudo[a]	1 $4e_2' \rightarrow 9e_1''$	2 $8a_1' \rightarrow 9e_1''$	3 $4e_2' \rightarrow 9e_1''$	4 $4e_2' \rightarrow 9e_1''$
Ref2(D_{5d})[f]		530	459	416	324
b3lyp/6-311++G(d,p)		570	491	367	276
b3lyp/6-311++G(d,p)	Lanl2dz	585	482	358	265
b3lyp/6-311G(d,p)	Lanl2dz	583	479	355	239
b3lyp/6-311G(d,p)		554	481	362	275
b3lyp/TZVP/DGDZVP2[b]		569	486	366	238
PBE0/6-311G(d,p)		501	457	345	223
PBE0/6-311G(d,p)	Lanl2dz	515	457	347	223
PBE0/6-311++G(d,p)	Lanl2dz	520	455	346	222
PBE0/6-311++G(d,p)		514	465	352	252
PBE0/6-311++G(d,p)[c]		503	457	347	251
PBE0/TZVP/DZVP[b]		542	480	359	228
PBE0/TZVP		542	480	359	229
PBE0/TZVP/DGDZVP2[b]		515	460	351	226
PBE0/TZVP/DGDZVP2[b,e]		526	469	353	228
PBE0/TZVP (PCM)[d]		543	481	360	229
PBE0/DGDZVP2 (PCM)		504	454	347	227
PBE0/aug-cc-pVTZ (PCM)[d]		521	476	358	247
PBE0/6-311G(d,p) (PCM)[d]		505	461	347	223
PBE0/6-311++G(d,p)[c] (PCM)[d]		502	458	347	247
b3lyp/6-311++G(d,p) (PCM)[d]	Lanl2dz	679	527	377	246
PBE/TZVP		432	406	338	279
PBE/TZVP/DGDZVP2[b]		417	396	331	272
PBE/TZVP		432	406	338	279
BPW91/TZVP		440	410	340	264
BPW91/TZVP (PCM)[d]		443	412	341	264
BPW91/6-311++G(d,p)	Lanl2dz	432	398	331	298

[a] Blank denotes full electron basis is used.
[b] The basis of iron is different from Cp's.
[c] The basis used in optimization step is 6-311G(d,p).
[d] The solvent is dichloro-methane, and the radii used is UAKS.
[e] In optimization step TZVP basis is used for all atoms.
[f] From Ref. [39].

Table 3
The excitation energies (unit: nm) of 18 low-level excited states of bis(benzene)chromium.

Calc.	Expr.[a,b]		Absolute error (in eV)
406	383		0.18
406	378		0.23
354	375	vs	−0.20
346	371	s	−0.25
346	367		−0.21
344	364	s	−0.19
344	361		−0.17
338	357		−0.19
338	353		−0.16
336	336		0.00
308	301		0.09
307	297		0.13
307	295		0.16
298	282		0.24
298	280	vs	0.27
298	278	s	0.30
297	276	b	0.32
297	276		0.32
280	273		0.11

[a] The signs in next column denote the strength of absorption band. vs, very strong; s, strong; b, broad.
[b] From Ref. [45].

3.4. Applications to other systems

Encouraged by the good agreement between experimental data and TDDFT calculation at PBE0/6-311++G(d,p) for ferrocene, we used this method to compute other systems. First we applied it to bis(benzene)chromium whose absorption spectra was obtained much early [45]. From the calculated result of bis(benzene)chromium (shown in Table 3), we can see that TD-PBE0/6-311++G(d,p) is of acceptable accuracy. But the error increases for higher excited states.

We further used TD-PBE0/6-311++G(d,p) to calculate eight low-level excitation energies of four derivatives of ferrocene. The result and the simulated UV–vis spectra and their comparisons with experimental values are given in Table 4. Table 4 shows little solvatochromism, or the solvent effect on absorption band is negligible. So we can use calculated values in vacuo for excitation spectra for this type of ferrocene derivatives. Secondly, we can see the deviations between theoretical and experimental values are usually smaller than 0.3 eV, which is consistent with the common error estimate for applying TDDFT to transition metal complexes. The mean error of our calculation is 24 nm (0.21 eV). But there are still larger deviations appearing on the third transition band in all of the four derivatives. For AcFc, for example, the deviation of that band is 0.46 eV. It is interesting to note that the deviation between theoretical and experimental value for the fourth absorption band is under 0.3 eV, much smaller than that of the third absorption band. This phenomenon may be possibly explained by the properties of the excited orbitals. To demonstrate this, we draw the orbital graphs of these molecules in Fig. 3. The third band excitation for these four derivatives including transitions, respectively, to the 62th orbital of AcFc, the 63th orbital of HyFc, the 57th orbital of ViFc, and the 59th orbital of EtFc. All these excited states have

deviations from experimental data. When PBE0 functional is employed, DZVP and 6-311G(d,p) basis are not accurate enough. However, using either 6-311++G(d,p) or DGDZVP2 basis can obtain more accurate acceptable result. Thus for metal complexes, we should use diffuse basis as suggested in Ref. [44].

Table 4
The eight low-level excitation energies and simulated absorption bands of four derivatives of ferrocene. The units are in nm.

	Calc.[a]	Calc. (PCM)	Oscillator strength[b]	Simulated[b]	Expr.	Err.[b] (eV)
AcFc	480.51	483.86	0.0004	483.00	450.00	−0.19
	467.26	468.32	0.0000			
	367.06	371.00	0.0012	370.00	360.00	−0.09
	355.70	357.54	0.0001			
	302.25	306.20	0.0014	297.00	334.00	0.46
	297.00	297.28	0.0068			
	279.35	285.57	0.0295	287.00	270.00	−0.27
	249.07	255.45	0.0035			
HyFc	465.98	475.52	0.0000	427.00	441.00	0.09
	462.84	468.39	0.0000			
	351.80	359.94	0.0000	332.00	322.00	−0.12
	350.77	354.29	0.0000			
	257.96	261.46	0.0004	252.00	270.00	0.33
	257.61	250.48	0.0000			
	242.01	234.44	0.0006			
	241.84	234.31	0.0003			
ViFc	474.24	476.14	0.0005	476.00	446.00	−0.18
	468.41	470.12	0.0000			
	359.91	361.05	0.0006	361.00	335.00	−0.27
	355.35	356.26	0.0000			
	280.05	281.30	0.0019	272.00	290.00	0.28
	270.13	271.48	0.0496			
	249.55	246.45	0.0035			
EtFc	473.27	475.21	0.0003	476.00	450.00	−0.15
	466.66	468.18	0.0000			
	358.45	359.87	0.0002	360.00	338.00	−0.22
	353.43	354.06	0.0000			
	259.07	261.41	0.0026	277.00	292.00	0.23
	248.76	250.46	0.0283			
	237.57	239.44	0.0000			
	234.32	237.98	0.1200			

[a] Calculated in vacuo.
[b] These data are obtained from PCM calculations.
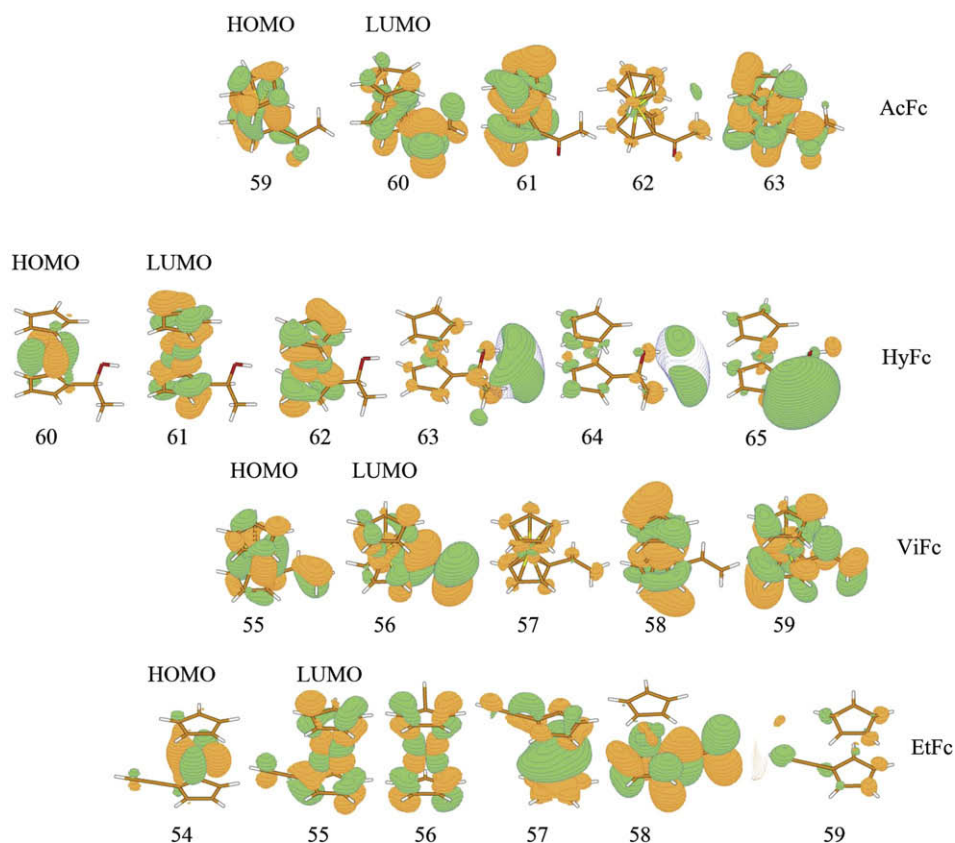
Fig. 3. HOMO, LUMO and some low-level virtual orbitals of the four derivatives of ferrocene.

more delocalized feature, and their accurate calculations are more difficult [38]. In contrast, the excited states of the fourth absorption band are relatively more localized and their calculated values are relatively more accurate.

We can also try to understand the feature of these absorption bands based on the analysis of orbitals. For example, the orbitals shown in Fig. 3 display obvious MLCT type of HOMO–LUMO transition. For the third band, the π–π^* feature is clear and it has larger oscillator strengths too. These features are similar to that of other ferrocene derivatives [7,46].

4. Conclusion

Some low levels of excitation energies of ferrocene have been calculated using TDDFT method with various combination of functionals and basis size. Our result shows that combined method of TD-PBE0/6-311++G(d,p) is a preferred choice for calculating absorption properties of metallocenes and their derivatives. Our study demonstrates that TD-PBE0 gives accurate absorption spectra of metallocenes.

Although the combination B3LYP/6-31G* is popular in all kinds of DFT calculations of properties of molecules, including TD-DFT calculations [2,4,6], the result in this Letter and from other studies [7,16] show that this combination could give erroneous result in calculations of excited state properties of molecules, especially for metallocenes and their derivatives. Alternatives are proposed by others, such as BPW91 [7]. Current study shows that the method TD-PBE0/6-311++G(d,p) can give accurate and reliable result for excited state calculations of metallocenes and their derivatives.

We also find that the calculated symmetry of virtual orbitals in TDDFT calculation can be different using different functionals, and more correct the symmetry is, more accurate the excited energies will be. Thus, it should be useful to check the correct symmetry of virtual orbitals after the optimized geometry has been obtained.

Since the derivatives of metallocenes are prototypes of more complex derivatives that have diverse utilities. We hope TD-PBE0/6-311++G(d,p) can be a good theoretical tool to study excited states of larger metal-containing systems, such as dye-sensitized photovoltaic solar-cells [47].

Acknowledgements

References

[1] K. Burke, J. Werschnik, E.K.U. Gross, J. Chem. Phys. 123 (2005) 062206.
[2] H.-Y. Xiao, Y.-J. Liu, W.-H. Fang, J. Mol. Struct.: THEOCHEM 802 (2007) 99.
[3] V. Wathelet, J.P. Michael, B.M. Fontaine, E.A. Perpete, J.-M. Andre, D. Jacquemin, Int. J. Quant. Chem. 106 (2006) 1853.
[4] C. Barolo et al., Inorg. Chem. 45 (2006) 4642.
[5] P. Boulet, H. Chermette, C. Daul, F. Gilardoni, F. Rogemond, J. Weber, G. Zuber, J. Phys. Chem. A 105 (2001) 885.
[6] W.-W. Zhang, Y.-G. Yu, Z.-D. Lu, W.-L. Mao, Y.-Z. Li, Q.-J. Meng, Organometallics 26 (2007) 865.
[7] V.N. Nemykin, A.Y. Maximov, A.Y. Koposov, Organometallics 26 (2007) 3138.
[8] P.L. Pauson, J. Organomet. Chem. 637 (2001) 3.
[9] I. Ciofini, P.P. Laine, F. Bedioui, C.A. Daul, C. Adamo, Comput. Rend. Chim. 9 (2006) 226.
[10] A. Rosa, G. Ricciardi, O. Gritsenko, E.J. Baerends, Struct. Bond. 112 (2004) 49.
[11] J. Danielsson, J. Ulicny, A. Laaksonen, J. Am. Chem. Soc. 123 (2001) 9817.
[12] L. Petit, P. Maldivi, C. Adamo, J. Chem. Theory Comput. 1 (2005) 953.
[13] B.O. Roos, Adv. Chem. Phys. 69 (1987) 399.
[14] K. Andersson, B.O. Roos, in: D.R. Yarkony (Ed.), Modern Electronic Structure Theory, World Scientific, 1995.
[15] T.H. Schucan, H. Weidenmuller, Ann. Phys. NY 73 (1972) 108.
[16] P. Joachim, M. Martijn, K. Georg, J. Chem. Phys. 127 (2007) 024103.
[17] F. Furche, K. Burke, Ann. Rep. Comput. Chem. 1 (2005) 20.
[18] A.D. McLean, G.S. Chandler, J. Chem. Phys. 72 (1980) 5639.
[19] Z.F. Xu, Y. Xie, W.L. Feng, H.F. Schaefer, J. Phys. Chem. A 107 (2003) 2716.
[20] G. Schreckenbach, J. Chem. Phys. 110 (1999) 11936.
[21] M.J. Frisch et al., GAUSSIAN 03, Revision A.1, Gaussian, Inc., Pittsburgh, PA, 2003.
[22] A.D. Becke, J. Chem. Phys. 98 (1993) 5648.
[23] J.P. Perdew, K. Burke, M. Ernzerhof, Phys. Rev. Lett. 77 (1996) 3865.
[24] J.P. Perdew, K. Burke, Y. Wang, Phys. Rev. B 54 (1996) 16533.
[25] C. Adamo, V. Barone, J. Chem. Phys. 110 (1999) 6158.
[26] A. Schaefer, C. Huber, R. Ahlrichs, J. Chem. Phys. 100 (1994) 5829.
[27] N. Godbout, D.R. Salahub, J. Andzelm, E. Wimmer, Can. J. Chem. 70 (1992) 560.
[28] T. Clark, J. Chandrasekhar, G.W. Spitznagel, P.V.R. Schleyer, J. Comput. Chem. 4 (1983) 294.
[29] A. Schafer, H. Horn, R. Ahlrichs, J. Chem. Phys. 97 (1992) 2571.
[30] Balabanov, K.A. Peterson, J. Chem. Phys. 123 (2005) 064107.
[31] T.H. Dunning Jr., P.J. Hay, in: H.F. Schaefer III (Ed.), Modern Theoretical Chemistry, vol. 3, Plenum, New York, 1976, p. 1.
[32] S. Miertus, J. Tomasi, Chem. Phys. 65 (1982) 239.
[33] S.I. Gorelsky, SWIZARD program, revision 4.5, <http://www.sg-chem.net/>.
[34] M.D. Rausch, A. Siegel, J. Organometal. Chem. 11 (1967) 317.
[35] M. Rosenblum, N. Brawn, J. Papenmiere, M. Applebaum, J. Organometal. Chem. 6 (1966) 173.
[36] A. Haaland, Acc. Chem. Res. 12 (1979) 415.
[37] C.M. Brett, B.E. Bursten, Polyhedron 23 (2004) 2993.
[38] A. Dreuw, M. Head-Gordon, Chem. Rev. 105 (2005) 4009.
[39] Y.S. Shon, D.N. Hendrickson, H.B. Gray, J. Am. Chem. Soc. 93 (1971) 3603.
[40] B. Kieron, W. Jan, E.K.U. Gross, J. Chem. Phys. 123 (2005) 062206.
[41] H.B. Gray, Y.S. Sohn, N. Hendrickson, J. Am. Chem. Soc. 93 (1971) 3603.
[42] S. Grimme, J. Phys. Chem. A 106 (2002) 6844.
[43] K. Ishimura, M. Hada, H. Nakatsuji, J. Chem. Phys. 117 (2002) 6533.
[44] J. Autschbach, F.E. Jorge, T. Ziegler, Inorg. Chem. 42 (2003) 2867.
[45] R.S. Berry, J. Chem. Phys. 35 (1961) 2025.
[46] V.N. Nemykin, E.A. Makarova, J.O. Grosland, R.G. Hadt, A.Y. Koposov, Inorg. Chem. 46 (2007) 9591.
[47] A. Hagefeldt, M. Gratzel, Chem. Rev. 95 (1995) 49.